Testing morphodynamic controls on the location and frequency of river avulsions on fans versus deltas: Huanghe (Yellow River), China

Vamsi Ganti[1], Zhongxin Chu[2], Michael P. Lamb[1], Jeffrey A. Nittrouer[3], and Gary Parker[4]

[1]Division of Geological and Planetary Sciences, California Institute of Technology, Pasadena, California, USA, [2]College of Marine Geosciences, Ocean University of China, Qingdao, China, [3]Department of Earth Science, Rice University, Houston, Texas, USA, [4]Department of Civil and Environmental Engineering and Department of Geology, Hydrosystems Laboratory, University of Illinois at Urbana-Champaign, Urbana, Illinois, USA

Abstract A mechanistic understanding of river avulsion location and frequency is needed to predict the growth of alluvial fans and deltas. The Huanghe, China, provides a rare opportunity to test emerging theories because its high sediment load produces regular avulsions at two distinct nodes. Where the river debouches from the Loess Plateau, avulsions occur at an abrupt decrease in bed slope and reoccur at a time interval (607 years) consistent with a channel-filling timescale set by the superelevation height of the levees. Downstream, natural deltaic avulsions reoccur at a timescale that is fast (7 years) compared to channel-filling timescale due to large stage-height variability during floods. Unlike the upstream node, deltaic avulsions cluster at a location influenced by backwater hydrodynamics and show evidence for episodic downstream migration in concert with progradation of the shoreline, providing new expectations for the interplay between avulsion location, frequency, shoreline rugosity, and delta morphology.

1. Introduction

Alluvial fans and deltas are dynamic, fan-shaped depositional landforms that develop where rivers emerge from mountainous regions to adjoining valleys, and where rivers enter a receiving basin of standing water, respectively. Alluvial fans and deltas are net depositional systems because both are characterized by spatially diminishing water surface slopes that reduce sediment transport capacity, thereby producing spatiotemporal convergence and deposition of sediment. Consequently, both features contribute to the stratigraphic record, and the deposits may be used to decipher past environmental conditions on Earth [e.g., *Bull*, 1977; *Humphrey and Heller*, 1995; *Whipple and Trayler*, 1996] and Mars [*Kleinhans*, 2005; *DiBiase et al.*, 2013]. Additionally, alluvial fans and river deltas are immensely valuable to society because of the natural resources that they offer: alluvial fans are a primary source of groundwater in arid and semiarid environments [*Listengarten*, 1984], and deltas host large populations and robust economies [*Vörösmarty et al.*, 2009]. A mechanistic understanding of fan and delta evolution will promote sustainability of these resources which are stressed by climatic change and anthropogenic activities and mitigate hazards by identifying areas prone to inundation from river floods and ocean storms [e.g., *Blum and Roberts*, 2009; *Syvitski and Saito*, 2007; *Syvitski et al.*, 2009]. Presently, we lack field examples to test models used to predict how fans and deltas evolve, especially in regard to the similarities and differences in processes contributing to their development.

Alluvial fans and deltas often develop planform fan shapes through avulsions, whereby major river channel shifts occur via "channel jumping" about a spatial node, rather than gradual channel migration [*Slingerland and Smith*, 2004]. Avulsion "set up" arises where a spatial decrease in water surface slope reduces sediment transport capacity, thus producing a spatial convergence in sediment flux and concomitantly generating in-channel sediment deposition [*Mohrig et al.*, 2000]. The avulsion "trigger" is typically an event whereby water flow leaves the channel (e.g., overbank flooding) and/or where erosion induces a levee-breach, during floods [e.g., *Edmonds et al.*, 2009; *Hajek et al.*, 2012]. While triggers are typically associated with flood events, the antecedent processes are critical to influencing the location and frequency of avulsions. For example, the measured avulsion timescale (T_{ma}), which is the time between two successive river avulsions, has been
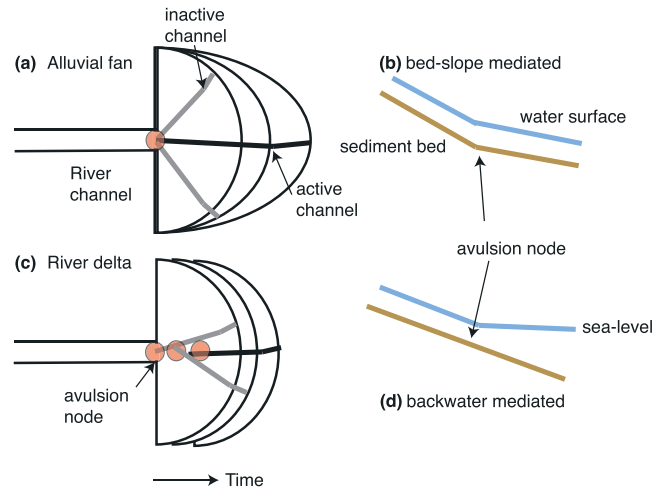
Figure 1. Schematic illustrating bed slope–mediated and backwater-mediated river avulsions. (a) A river channel feeding sediment and water to an alluvial fan or fan delta, where avulsions occur at a spatially fixed node and the fan grows outward in time from its uplands source. (b) bed slope–mediated river avulsions occur due to the topographic slope break, which reduces water surface slope and sediment transport capacity. (c) A river channel feeding sediment and water to a receiving basin of standing water, where avulsion node migrates seaward in step with shoreline progradation. (d) Backwater-mediated river avulsions result from dynamic backwater effects.

proposed to scale with characteristic channel-filling timescale (T_c), i.e., the time it takes for the riverbed to aggrade by a characteristic height Δz:

$$T_c = \Delta z / v_a , \quad (1)$$

where v_a is the mean vertical aggradation rate and Δz is the characteristic channel depth, h_c [e.g., *Bryant et al.*, 1995; *Jerolmack and Mohrig*, 2007; *Jerolmack*, 2009; *Reitz and Jerolmack*, 2012]. For comparison, we define a dimensionless avulsion timescale as the ratio of the measured and expected avulsion timescales:

$$T_a^* = T_{ma} / T_c \quad (2)$$

in which T_a^* is thought to be order unity. For low-sloping rivers others have argued that Δz in equation (1) is more appropriately characterized by the superelevation height of the channel levees with respect to the floodplain [e.g., *Mackey and Bridge*, 1995; *Heller and Paola*, 1996; *Mohrig et al.*, 2000; *Hajek and Wolinsky*, 2012]. In addition, experiments suggest that the duration of levee-breaching flows can be an important factor in setting the frequency and location of river avulsions [*Edmonds et al.*, 2009].

On alluvial fans and fan deltas, channel filling is thought to be focused where upland channel confinement ceases (e.g., at a canyon-fan transition) so that channel bed and water surface slopes reduce, producing a lower sediment transport capacity [e.g., *Blair and McPherson*, 1994; *Jones and Schumm*, 1999; *Slingerland and Smith*, 2004]. A consequence is in-channel sediment aggradation and the increased likelihood of avulsion [*Parker et al.*, 1998]. Alluvial fans and fan deltas therefore typically have an avulsion node that is topographically pinned, whereby fan deposits grow outward in time from their confined upland source. We term this type of avulsion a "bed slope–mediated" avulsion (Figures 1a and 1b).

Alternatively, through routine avulsions at a fixed spatial node, river-dominated deltas often produce arcuate planform morphologies similar to alluvial fans and fan deltas without an obvious change in topographic confinement or channel bed slope (Figures 1c and 1d). Instead, avulsions on deltas appear to occur within a region of high water surface slope variability caused by backwater hydrodynamics, where the length of the backwater zone measured upstream from the shoreline scales approximately with,

$$L_b = h_c / S, \quad (3)$$

in which S is the channel bed slope [e.g., *Jerolmack and Swenson*, 2007; *Jerolmack*, 2009]. The backwater zone is characterized by spatial flow deceleration and deposition at low flows, and flow acceleration and bed scour at high flows [*Nittrouer et al.*, 2012; *Lamb et al.*, 2012; *Chatanantavet and Lamb*, 2014], and this transient behavior is thought to set the locus for avulsion on deltas [*Chatanantavet et al.*, 2012]. We term these avulsions "backwater-mediated" river avulsions.

The differences between the hypothesized processes influencing fan and delta avulsions are significant. For example, given sufficient sediment supply, alluvial fans and fan deltas may grow indefinitely in size through repeated avulsions about a node fixed spatially by topography. However, given the backwater-mediated avulsion hypothesis, deltas cannot grow indefinitely in size (defined as the distance between the avulsion node and shoreline), because slope and depth are held roughly constant provided relatively consistent upstream feeds of water and sediment [e.g., *Parker*, 2004]. Instead, delta lobes reach a maximum size that is set by L_b [*Jerolmack*, 2009], so that delta progradation must occur with commensurate advance of the delta avulsion node (Figures 1c and 1d).

River avulsions occur infrequently in natural systems; therefore, most tests of these aforementioned hypotheses come from laboratory experiments, and limited field data [e.g., *Bryant et al.*, 1995; *Jerolmack and Mohrig*, 2007; *Reitz and Jerolmack*, 2012]. Additional field data from active systems are needed to test the scaling relationships that predict the location and frequency of river avulsions for fans and deltas. Herein we use the rich historical data from the Huanghe (Yellow River), China, which provide an unprecedented case study because this river system has until recently carried the third largest sediment load for rivers worldwide [*Milliman and Syvitski*, 1992]. This condition produced rapid shoreline progradation and frequent avulsions at two distinct avulsion nodes.

2. Study Area: Lower Huanghe

The Huanghe is the second largest river basin in China, draining a total area of 752,443 km^2 over its 5464 km length [*Saito et al.*, 2000]. Over the last 2000 years, the sediment discharge was ~1–1.1 × 10^9 t/yr [*Milliman and Syvitski*, 1992]. Since 1855, delta progradation rates averaged ~150 m/yr [*van Gelder et al.*, 1994]. Additionally, due to high in-channel sedimentation rates (centimeters per year) [*van Gelder et al.*, 1994], the system is prone to frequent avulsions; in the last 5000 years the river has shifted course at least 26 times [*Saito et al.*, 2000; *Pang and Si*, 1979]. The uniqueness of the Huanghe in terms of sediment load necessitates engineered avulsions, which have been ongoing since 1930; our analysis neglects man-made avulsions and focuses on the historical record pre-1930.

The Huanghe possesses two distinct avulsion nodes that we hypothesize coincide with the bed slope–mediated and backwater-mediated locations. The former is located in the vicinity of Huayuankou, roughly 700 km upstream of the modern shoreline, which is near where the river exits the Loess Plateau. Excluding the engineered avulsion disaster of 1938, the last major avulsion at the Huayuankou node occurred in 1855, and this event directed the Huanghe along its present course to the Bohai Sea [*Saito et al.* [2000]] (Figure 2a). The latter node is located in the vicinity of Lijin (Figure 2), roughly 70 km upstream of the modern shoreline, which corresponds to the apex of the modern delta.

3. Location of River Avulsions

Figure 2a shows the map of historical avulsions at the Huayuankou (upstream) avulsion node [after *Saito et al.*, 2000] where the river has avulsed 10 times in the past 5000 years. We extracted the long profile of the lower Huanghe (Figure 2c) from the Shuttle Radar Topography Mission data (spatial resolution: 3 arc sec, ~90 m). The topographic long profile shows a tenfold change in bed slope upstream of the Huayuankou location (from $S = 1.3 \times 10^{-3}$ at 960 km to $S = 2.0 \times 10^{-4}$ at 760 km; Figure 1b). This change in slope, which corresponds to a transition from Loess Plateau uplands to the North China Plain, produces an order of magnitude decrease in the sediment transport capacity (section 1 in Text S1 in the supporting information), and thus in-channel sedimentation that spatially coincides with major, historical river avulsions [e.g., *van Gelder et al.*, 1994; *Chu et al.*, 2006]. Furthermore, avulsions have been spatially consistent for the last 5000 years despite significant progradation of the fan (Figure 2a). These observations suggest that avulsions at Huayuankou are driven by changes in bed slope.

Figure 2b shows a map of historical avulsions near Lijin [after *Pang and Si*, 1979; *Chu et al.*, 2006], where seven natural avulsions occurred between 1855 and 1930 [*Pang and Si*, 1979]. Unlike the upstream bed slope–mediated avulsion node, there is no coincident topographic slope break near Lijin (Figure 2c). We measured the streamwise distances of the avulsion nodes (Figure 2b) from a fixed reference point: Lijin (Figures 3a and S1 and section 2 in Text S1). Shoreline progradation, measuring 0.12 ± 0.07 km/yr since 1855, is quantified by computing the average radial distance of past shorelines from Lijin (Figures 2b and 3a) [*Pang and Si*, 1979; *Chu et al.*, 2006]. Although there is significant variability in the data, our analysis indicates that, on average, this avulsion node migrated seaward (Figure 3a) by a rate of 0.18 ± 0.02 km/yr (section 2 in Text S1).

The temporal evolution of the deltaic avulsion site is not consistent with the model of a fixed avulsion location, but interestingly this node also does not display continuous seaward migration, as might be expected for backwater-mediated avulsions on a radially symmetric delta (Figure 1c). For example, the avulsions in 1889, 1904, and 1929 occurred at roughly the same location, while other avulsions during the
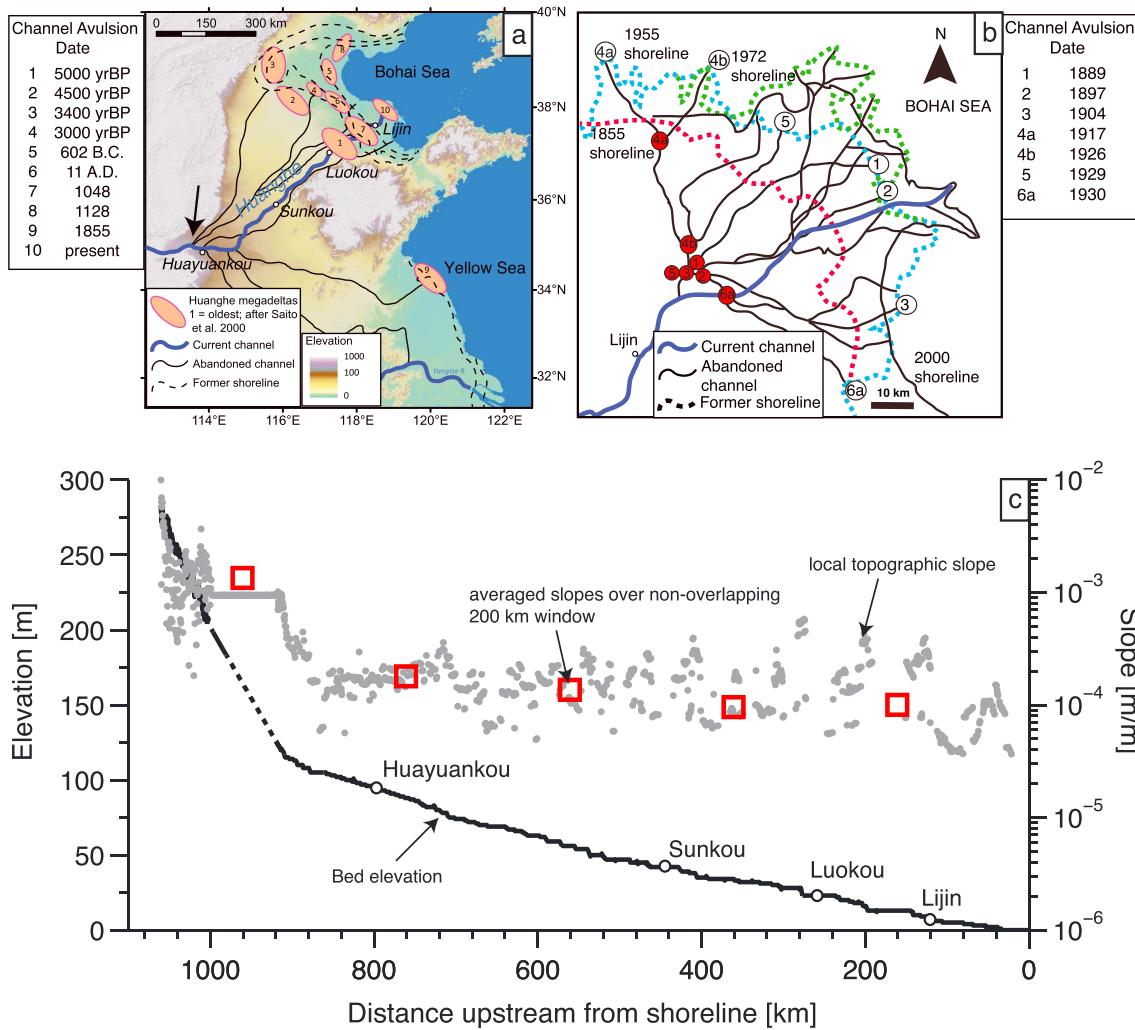
Figure 2. (a) Map showing the historical river avulsions on the Huanghe [after *Saito et al.*, 2000]. (b) Map of the deltaic avulsions on Huanghe from 1855 to 1930. Red circles indicate avulsion nodes, dashed lines indicate paleoshorelines, and white circles are the river mouths at the time of avulsion [after *Pang and Si*, 1979; *Chu et al.*, 2006]. (c) Topographic long profile of the Lower Huanghe (solid black line) along with the local topographic slope (gray markers). The dashed line indicates where a dam exists and the data were linearly interpolated.

period 1855–1930 occurred farther downstream. Thus, while the data support migration of the avulsion node in concert with shoreline progradation, node migration has occurred episodically.

To further test the hypothesized backwater control on delta avulsion location, we computed the characteristic backwater length $L_b = h_c / S$ using the channel bed slope in the lower Huanghe reaches, from Luokou to Lijin (Figure 2c), measured over the last 70 years (8.8×10^{-5} to 1.0×10^{-4}) [*United Nations Educational, Scientific and Cultural Programme International Sedimentation Initiative*, 2005]. Historically, the bankfull flow depth at Lijin varied from 2 to 5 m [e.g., *van Gelder et al.*, 1994; *Wu et al.*, 2005; *Wang et al.*, 2013]. We used this range to yield an estimated backwater length of 21–54 km. Measured upstream of the shoreline, this predicted distance corresponds to the location of avulsions (Figure 3a); avulsions consistently occurred within the backwater zone of the Huanghe, providing support for the backwater-mediated avulsion hypothesis.

4. Timescales of River Avulsions

Here we analyze if the two Huanghe avulsion nodes produce different characteristic avulsion timescales. Using historical records [*Saito et al.*, 2000; *Pang and Si*, 1979], the observed mean and standard error of avulsion timescales at the bed slope–mediated and the backwater-mediated nodes are $T_{ma} = 607 \pm 121$ years
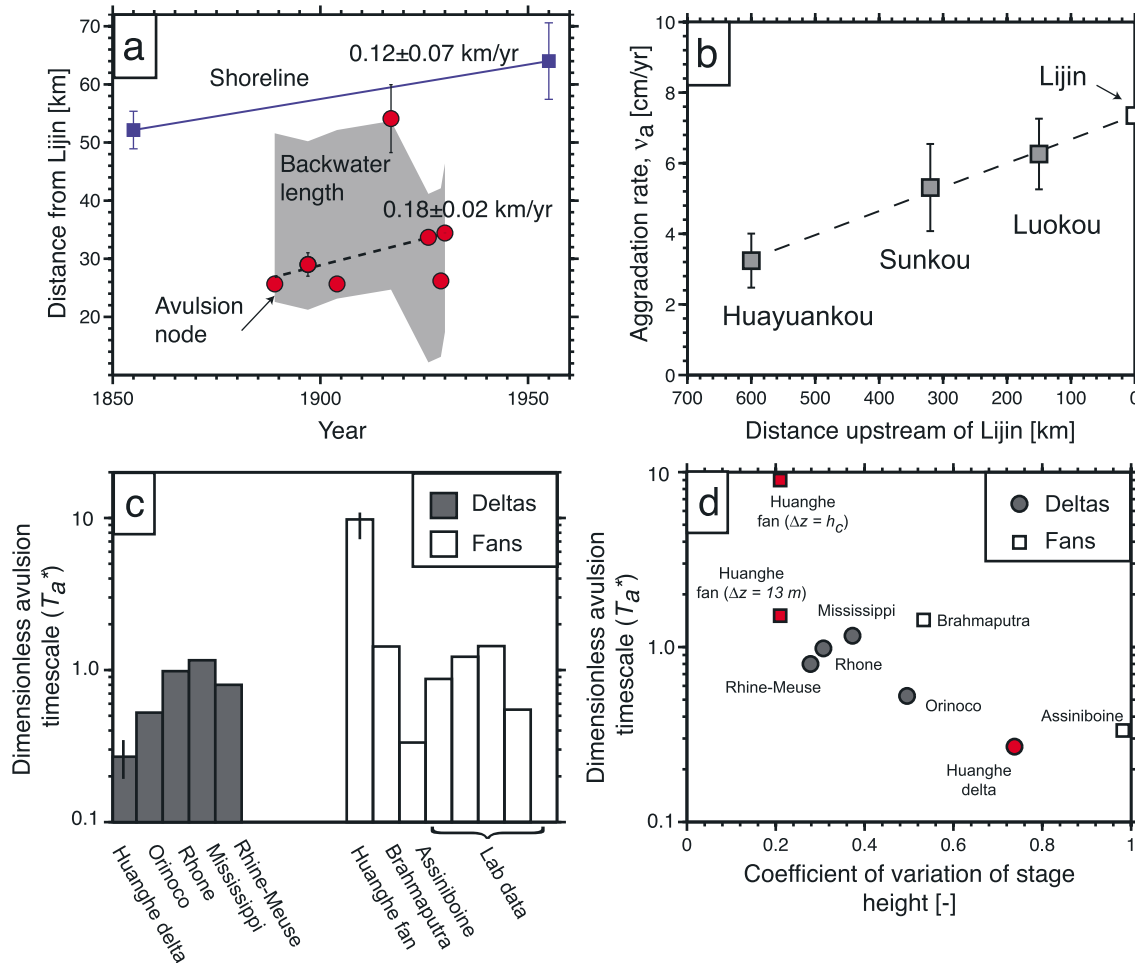
Figure 3. (a) Evolution of the shoreline (blue squares), measured as the average radial distance from Lijin. The distance of the avulsion node (red circles) from Lijin was measured along the river (where not shown, the error bars are smaller than the symbol size). The shaded area denotes the predicted range of distances of the avulsion node computed by subtracting the backwater length (21–54 km) from the streamwise distance of the shoreline from Lijin. The dashed black line indicates the best fit line to the temporal evolution of the backwater-mediated avulsion nodes. (b) Computed vertical mean aggradation rates (and standard error) from historical cross-sectional data (Figure S2) at three sites along the Huanghe, along with the best fit line (dashed black line). (c) Comparison of the dimensionless avulsion timescale (equation (2); T_a^*) at the bed slope–mediated and backwater-mediated avulsion nodes of the Huanghe. Gray and white bars correspond to deltas and alluvial fans, respectively. Note that downscaling and large Froude numbers in physical experiments likely produce bed slope–mediated avulsion nodes rather than backwater-mediated avulsion nodes, making them closer analogs to steep, coarse grained fan deltas rather than deltas built by large, low-gradient rivers [e.g., *Sheets et al.*, 2007]. (d) Comparison of T_a^* with the coefficient of variation of the water stage-height for the natural deltas and fans compiled in Figure 3c (section 4 in Text S1). For all the rivers on this plot (apart from additional Huanghe fan data point), T_c is computed using the characteristic channel depth as the Δz metric (equation (1)).

and 7 ± 2 years, respectively. To compute the characteristic channel-filling timescale, T_c (equation (1)), we compute the mean in-channel aggradation rates (v_a) using historical cross-sectional data (Figure S2) measured for the Huanghe at three sites: Huayuankou, Sunkou (~300 km upstream of Lijin), and Loukou (~150 km upstream of Lijin) (Figure 2a). The active channel for each cross section is identified (Text S1), and the elevation data for the 1950s and 2001 are differenced and averaged (Figure S2 and section 3 in Text S1). Our results indicate that channel aggradation rates increase downstream (Figure 3b). We use a linear extrapolation to infer the vertical aggradation rate at Lijin as ~7.5 cm/yr (cross-sectional profiles were not available at Lijin), and characteristic flow depth of 2 m at both avulsion sites (consistent with observations of bankfull depths at Lijin and Huayuankou) [*Ma et al.*, 2012; *Wang et al.*, 2013].

Our analyses indicate that the channel-filling timescale $T_c = 62$ years at the bed slope–mediated avulsion node (where $h_c = 2$ m and $v_a = 3.24$ cm/yr) is significantly smaller than measured avulsion time $T_{ma} = 607$ years (i.e., $T_a^* = 9$) (Figure 3c). In contrast, $T_c = 27$ years at the backwater-mediated avulsion node (where $v_a = 7.5$ cm/yr) is significantly greater than $T_{ma} = 7$ years (i.e., $T_a^* = 0.26$).

5. Discussion

5.1. Channel-Filling Timescale Versus Avulsion Timescale

The calculation for channel-filling timescale (T_c) is higher than the measured avulsion timescale (T_{ma}) at the Huanghe delta and lower at the upstream fan. To compare these values to other field localities, $T_a{}^*$ estimates for six modern delta and fan systems and four experimental fans were compiled from *Jerolmack and Mohrig* [2007]. The $T_a{}^*$ values (Figure 3c) show no systematic trends for the fans or deltas, although our calculations of $T_a{}^*$ for the Huanghe depart strongly from the other systems. Because there appears to be no systematic difference in $T_a{}^*$ between fans and deltas, in general, we need an alternate explanation for the variability in $T_a{}^*$ at the Huanghe.

At the bed slope–mediated avulsion node, $T_a{}^*$ would equal unity if the characteristic length (Δz) is increased to 7–9h_c (equation (1)). Coincidently, 7–9h_c is similar to the superelevation height of channel levees (13 m) with respect to the adjacent floodplain [*Chen et al.*, 2011]. This suggests that superelevation height of levees, rather than channel depth, might be the more appropriate length scale in equation (1) [e.g., *Heller and Paola*, 1996; *Mohrig et al.*, 2000]. At the backwater-mediated avulsion node, $T_a{}^* < 1$ also could be due to underestimating the aggradation rate at Lijin because our linear extrapolation from upstream sites (Figure 3b) does not account for backwater hydrodynamics that can enhance deposition rates [e.g., *Nittrouer et al.*, 2012].

In addition, water stage-height variability may play a key role in determining avulsion reoccurrence time by affecting the channel-filling processes via backwater hydrodynamics [e.g., *Chatanantavet et al.*, 2012] that result in an avulsion set up, and by determining the frequency and magnitude of overbank flows which serve as the avulsion trigger [e.g., *Slingerland and Smith*, 2004]. For example, *Edmonds et al.* [2009] showed that avulsions occurred in an experimental delta in areas with prolonged and frequent overbank flows. To evaluate these hypotheses we compiled water stage-height variability for seven rivers and found that the water stage variability for the Huanghe delta node is substantially higher than the other river systems, which may additionally explain low values of $T_a{}^*$ there (Figures 3d, S3 and S4 and section 4 in Text S1). In addition, water stage-height variability is relatively small at the upstream bed slope–mediated node of the Huanghe, which may in turn explain high $T_a{}^*$ there.

5.2. Location of Backwater-Mediated Avulsion Nodes

For radially symmetric deltas, models for deltaic evolution require that avulsions controlled by backwater hydrodynamics migrate downstream with shoreline progradation (e.g., Figure 1) [*Jerolmack*, 2009]; these models are largely untested. Although there is a statistically significant trend of downstream migration of the backwater-mediated avulsion node of the Huanghe (Figure 3a), this migration is not monotonic over avulsion timescales nor does the shoreline maintain precise radial symmetry. Instead, the delta is built through construction of lobes that produce shoreline rugosity (e.g., Figure 2b) [*Reitz and Jerolmack*, 2012], which we propose results in temporally and spatially variable backwater lengths that affect avulsion locations. For example, the avulsion node location may stay relatively fixed as multiple lobes preferentially fill in topographic lows [e.g., *Straub et al.*, 2009] until the distance between the avulsion node and the shoreline is everywhere greater than L_b (Figure 4). At this point, we expect the avulsion node to jump seaward with farther shoreline progradation, and the magnitude of this jump depends on the distance a typical delta lobe protrudes from the radially averaged shoreline.

We can estimate the characteristic scale of delta lobe protrusion from the radially averaged shoreline (D) just prior to avulsion as

$$D = PT_{ma}, \tag{4}$$

in which P is the progradation rate of the delta lobe (Figure 4). Although coastal erosion and deposition due to waves, tides, and currents may also affect lobe progradation, for simplicity we focus on river-dominated deltas. For a prograding delta with constant sea level and no subsidence, $P \approx v_a/S$ (e.g., Figure 4a) [*Paola*, 2000], so that equation (4), combined with equations (1)–(3) can be rewritten as

$$D = L_b T_a{}^*. \tag{5}$$

Equation (5) shows that the characteristic scale of delta lobe protrusion from the radially averaged shoreline scales with the backwater length (L_b) and dimensionless avulsion timescale ($T_a{}^*$), indicating that avulsion location, frequency and shoreline rugosity are all interrelated.
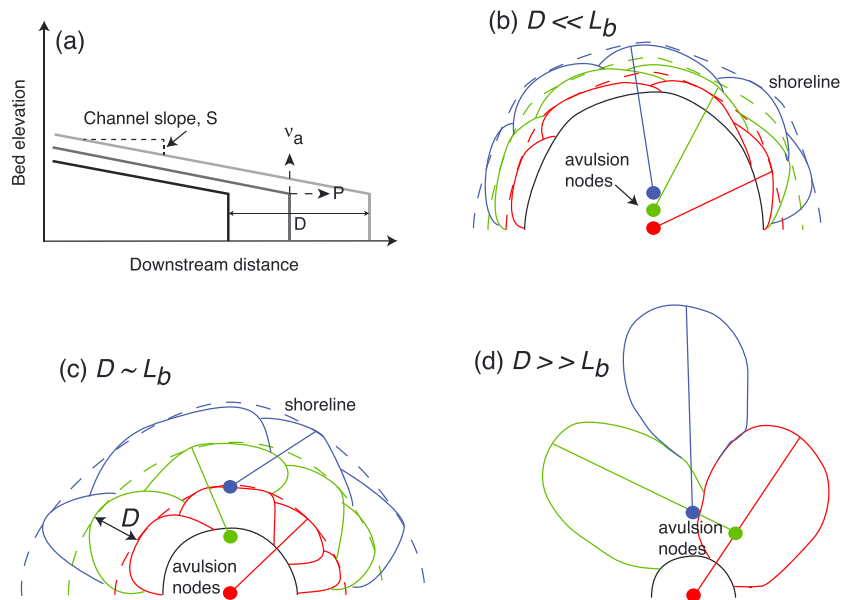
Figure 4. (a) Idealized schematic of 1-D bed elevation of a river channel under constant sea level and no subsidence in which shoreline progradation (P) results in aggradation (v_a). (b) When the length scale of progradation (D) is much smaller than the backwater length (L_b), the backwater-mediated avulsion sites likely exhibit gradual seaward migration over multiple avulsion timescales and the shoreline shows minimal deviation from the idealized radially symmetric shape. (c) When D is on the same scale as L_b, the backwater-mediated avulsion sites are likely to make large jumps seaward episodically and the shoreline is rugose. (d) When D is much larger than L_b, the backwater-mediated avulsion sites likely migrate downstream with each avulsion. The outline colors of the delta lobes match the color of the avulsion node (solid circles) from where the channel progrades, namely, lobes outlined with blue color correspond to avulsions at the blue avulsion node.

Three distinct cases arise: (1) if $D \ll L_b$ (i.e., $T_a^* \ll 1$), then lobe protrusion (D) is small compared to lobe size (L_b), the shoreline appears relatively smooth, and repeated avulsions result in progradation of a nearly radially symmetric delta (Figure 4b). At the point when the distance between the avulsion node and the shoreline is everywhere greater than L_b, the avulsion node must migrate seaward by a distance of $\sim D$, which in this case is small compared to the delta size ($\sim L_b$), resulting in avulsion node migration that occurs in "fits and starts" but follows an overall gradual trend of downstream migration (Figure 4b). (2) If $D \approx L_b$ ($T_a^* \approx 1$), then the shoreline is rugose, and the backwater-mediated avulsion node is likely to episodically jump seaward at the scale of the delta itself ($D \approx L_b$). Avulsions are again spatially grouped until the shoreline progrades everywhere past a distance L_b from the previous avulsion node (Figure 4c). And (3) if $D \gg L_b$ (i.e., $T_a^* \gg 1$), then the backwater-mediated avulsion node migrates seaward significantly with each avulsion (Figure 4d), in which case the delta is more likely to exhibit an elongated planform geometry.

For the Huanghe, the axial plane of the backwater-mediated avulsions exhibits downstream migration on the same scale as the deviation of the shoreline from radial symmetry (Figure 2b), indicating that this avulsion node is likely to migrate seaward episodically. Moreover, our compilation (Figure 3c) suggests that $T_a^* \approx 1$ (and therefore, $D \approx L_b$ according to equation (5)) for various deltas. Thus, deltas with rugose shorelines and delta lobe-scale jumps in the avulsion location (i.e., Figure 4c) are likely to be common. Rising sea level or subsidence would lower delta progradation rates [e.g., *Jerolmack*, 2009] and the avulsion timescales from what we considered here, resulting in more symmetric deltas (smoother shorelines) that would promote gradual avulsion node migration (Figure 4b).

Despite jumps in the avulsion node location, our results indicate that delta lobe size (measured as the distance from the avulsion node to the shoreline) may remain constant during delta evolution. This provides a guideline for the most likely location for future avulsions, which has important implications for evaluating the vulnerability and sustainability of infrastructure built on deltaic landscapes. In addition, these results support the use of backwater length scaling for paleohydraulic analysis [e.g., *DiBiase et al.*, 2013] where delta lobe size, flow depth, and slope are related (i.e., $L_b = h_c/S$).

6. Conclusions

Our work provides field testing of the idea that river avulsions on alluvial fans and deltas arise due to different controls on water surface slope. Analysis of the Huanghe is consistent with the hypothesis that bed slope–mediated avulsion sites are driven by a topographic slope break, which produces an alluvial fan (or fan delta) that can grow without impedance. Additionally, backwater-mediated avulsions are driven by hydrodynamics near a receiving basin of standing water, where the delta lobe size is consistent, and the avulsion node migrates downstream commensurate with the shoreline progradation. However, we find that the seaward migration of the backwater-mediated avulsion node is likely episodic and is linked to shoreline rugosity, delta lobe size, and the dimensionless avulsion timescale. Finally, we find that the dimensionless avulsion timescale is not systematically different between fans and deltas and that stage-height variability may play an important role in setting the frequency of avulsions.

References

Blair, T. C., and J. G. McPherson (1994), Alluvial fans and their natural distinction from rivers based on morphology, hydraulic processes, sedimentary processes, and facies assemblages, *J. Sediment. Res.*, *A64*(3), 450–489.

Blum, M. D., and H. H. Roberts (2009), Drowning of the Mississippi delta due to insufficient sediment supply and global sea-level rise, *Nat. Geosci.*, *2*, 488–491.

Bryant, M., P. Falk, and C. Paola (1995), Experimental study of avulsion frequency and rate of deposition, *Geology*, *23*, 365–368.

Bull, W. B. (1977), The alluvial fan environment, *Prog. Phys. Geogr.*, *1*, 222–270.

Chatanantavet, P., and M. P. Lamb (2014), Sediment transport and topographic evolution of a coupled river and river plume system: An experimental and numerical study, *J. Geophys. Res. Earth Surf.*, *119*, 1263–1282, doi:10.1002/2013JF002810.

Chatanantavet, P., M. P. Lamb, and J. A. Nittrouer (2012), Backwater controls on avulsion location on deltas, *Geophys. Res. Lett.*, *39*, L01402, doi:10.1029/2011GL050197.

Chen, Y., I. Overeem, J. P. M. Syvitski, S. Gao, and A. J. Kettner (2011), *Controls on Levee Breaches on the Lower Yellow River During the Years 1550–1855*, pp. 617–633, RCEM publication, Tsinghua Univ. Press, Beijing.

Chu, Z. X., X. G. Sun, S. K. Zhai, and K. H. Xu (2006), Changing pattern of accretion/erosion of the modern Yellow River (Huanghe) subaerial delta, China: Based on remote sensing images, *Mar. Geol.*, *227*, 13–30.

DiBiase, R. A., A. B. Limaye, J. S. Scheingross, W. W. Fischer, and M. P. Lamb (2013), Deltaic deposits at Aeolis Dorsa: Sedimentary evidence for a large body of water in the northern plains of Mars, *J. Geophys. Res. Planets*, *118*, 1285–1302, doi:10.1002/jgre.20100.

Edmonds, D. A., D. C. J. D. Hoyal, B. A. Sheets, and R. L. Slingerland (2009), Predicting delta avulsions: Implications for coastal wetland restoration, *Geology*, *37*, 759–762.

Hajek, E., and M. A. Wolinsky (2012), Simplified process modeling of river avulsions and alluvial architecture: Connecting models and field data, *Sediment. Geol.*, *257-260*, 1–30, doi:10.1016/j.sedgeo.2011.09.005.

Hajek, E., P. Heller, and E. Schur (2012), Field test of autogenic control on alluvial stratigraphy (Ferris Formation, Upper Cretaceous-Paleogene, Wyoming), *Geol. Soc. Am. Bull.*, *124*(11–12), 1898–1912.

Heller, P. L., and C. Paola (1996), Downstream changes in alluvial architecture: An exploration of controls on channel-stacking patterns, *J. Sediment. Res.*, *66*(2), 297–306.

Humphrey, N. F., and P. L. Heller (1995), Natural oscillations in coupled geomorphic systems: An alternative origin for cyclic sedimentation, *Geology*, *23*(6), 499–502.

Jerolmack, D. J. (2009), Conceptual framework for assessing the response of delta channel networks to Holocene sea level rise, *Quat. Sci. Rev.*, doi:10.1016/j.quascirev.2009.02.015.

Jerolmack, D. J., and D. Mohrig (2007), Conditions for branching in depositional rivers, *Geology*, *35*(5), 463–466.

Jerolmack, D. J., and J. Swenson (2007), Scaling relationships and evolution of distributary networks on wave-influenced deltas, *Geophys. Res. Lett.*, *34*, L23402, doi:10.1029/2007GL031823.

Jones, L. S., and S. A. Schumm (1999), Causes of avulsion: An overview, in *Fluvial Sedimentology VI*, Special Publication of the International Association of Sedimentologists 28, edited by N. D. Smith and J. Rogers, pp. 171–178, Blackwell, Oxford, U. K.

Kleinhans, M. G. (2005), Flow discharge and sediment transport models for estimating a minimum timescale of hydrological activity and channel and delta formation on Mars, *J. Geophys. Res.*, *110*, E12003, doi:10.1029/2005JE002521.

Lamb, M. P., J. Nittrouer, D. Mohrig, and J. Shaw (2012), Backwater and river-plume controls on scour upstream of river mouths: Implications for fluvio-deltaic morphodynamics, *J. Geophys. Res.*, *117*, F01002, doi:10.1029/2011JF002079.

Listengarten, V. A. (1984), Alluvial cones as deposits of groundwater, *Int. Geol. Rev.*, *26*, 168–177.

Ma, Y., H. Q. Huang, G. C. Nanson, Y. Li, and W. Yao (2012), Channel adjustments in response to the operation of large dams: The upper reach of the lower Yellow River, *Geomorphology*, *147–148*, 35–48.

Mackey, S. D., and J. S. Bridge (1995), Three-dimensional model of alluvial stratigraphy: Theory and application, *J. Sediment. Res.*, *65*, 7–31.

Milliman, J. D., and J. P. M. Syvitski (1992), Geomorphic/tectonic control of sediment discharge to the oceans: The importance of small mountain rivers, *J. Geol.*, *100*, 525–544.

Mohrig, D., P. L. Heller, C. Paola, and W. J. Lyons (2000), Interpreting avulsion process from ancient alluvial sequences: Guadalope-Matarranya system (northern Spain) and Wasatch Formation (western Colorado), *Geol. Soc. Am. Bull.*, *112*(12), 1787–1803.

Nittrouer, J. A., J. Shaw, M. P. Lamb, and D. Mohrig (2012), Spatial and temporal trends for water-flow velocity and bed-material transport in the lower Mississippi River, *Geol. Soc. Am. Bull.*, doi:10.1130/B30497.1.

Pang, J. Z., and S. H. Si (1979), Evolution of the Yellow River mouth: I. Historical shifts, *Oceanologia et Limnologia Sinica*, *10*(2), 136–141.

Paola, C. (2000), Quantitative models for sedimentary basin filling, *Sedimentology*, *47*, 121–178.

Parker, G. (2004), 1D Sediment transport morphodynamics with applications to rivers and turbidity currents, E-book. [Available at http://hydrolab.illinois.edu/people/parkerg/morphodynamics_e-book.htm.]

Parker, G., C. Paola, K. X. Whipple, and D. Mohrig (1998), Alluvial fans formed by channelized fluvial and sheet flow. I: Theory, *J. Hydraul. Eng.*, *124*(10), 985–995.

Reitz, M. D., and D. J. Jerolmack (2012), Experimental alluvial fan evolution: Channel dynamics, slope controls, and shoreline growth, *J. Geophys. Res.*, *117*, F02021, doi:10.1029/2011JF002261.

Saito, Y., H. Wei, Y. Zhou, A. Nishimura, Y. Sato, and S. Yokota (2000), Delta progradation and chenier formation in the Huanghe (Yellow River) delta, China, *J. Asian Earth Sci.*, *18*, 489–497.

Sheets, B. A., C. Paola, and J. M. Kelberer (2007), Creation and preservation of channel-form sand bodies in an experimental alluvial basin, in *Sedimentary Processes, Environments and Basins*, edited by G. Nichols, E. Williams, and C. Paola, pp. 555–567, Blackwell, Oxford, U. K.

Slingerland, R., and N. D. Smith (2004), River avulsions and deposits, *Annu. Rev. Earth Planet. Sci.*, *32*, 257–285, doi:10.1146/annurev. earth.32.101802.120201.

Straub, K. M., C. Paola, D. Mohrig, M. A. Wolinsky, and T. Geroge (2009), Compensational stacking of channelized sedimentary deposits, *J. Sediment. Res.*, *79*(9), 673–688.

Syvitski, J. P., and Y. Saito (2007), Morphodynamics of deltas under the influence of humans, *Global Planet. Change*, *57*(3), 261–282.

Syvitski, J. P. M., et al. (2009), Sinking deltas due to human activities, *Nat. Geosci.*, *2*, 681–686.

United Nations Educational, Scientific and Cultural Organization-International Hydrological Programme International Sedimentation Initiative (2005), Case study on the Yellow River sedimentation, *International Research and Training Center on Erosion and Sedimentation*, Beijing, China, pp. 132, Nov.

van Gelder, A., J. H. van den Berg, G. Cheng, and C. Xue (1994), Overbank and channelfill deposits of the modern Yellow River delta, *Sediment. Geol.*, *90*, 293–305.

Vörösmarty, C. J., J. P. M. Syvitski, J. Day, A. de Sherbinin, L. Giosan, and C. Paola (2009), Battling to save the world's river deltas, *Bull. Atomic Scientists*, *65*(2), 31–43.

Wang, Y., X. Fu, Y. Zhnag, and G. Parker (2013), Temporal change in bankfull characteristics of the Yellow River: Single-thread versus multiple-thread reach, in *Proceedings of 2013 IAHR Congress*, Tsinghua Univ. Press, Beijing.

Whipple, K. X., and C. R. Trayler (1996), Tectonic control on fan size: The importance of spatially variable subsidence rates, *Basin Res.*, *8*, 351–366.

Wu, B., G. Wang, J. Ma, and R. Zhang (2005), Case study: River training and its effects on fluvial processes in the lower Yellow River, China, *J. Hydraul. Eng.*, *31*(2), 85–96.